^{125}I seeds irradiation inhibits tumor growth and induces apoptosis by Ki-67, P21, Survivin、Livin and Caspase-9 expression in lung carcinoma xenografts

Lijun Wang (wlj20190211@163.com)
Affiliated Hospital of Medical College Qingdao University
Cunzhi Lin
Affiliated Hospital of Medical College Qingdao University
Qing Jin
The 903th Hospital of PLA joint logistics support force
Xinhong Zhu
Qingdao Municipal Hospital Group
Yiwei Cao
Affiliated Hospital of Medical College Qingdao University
Caihong Guo
Affiliated Hospital of Medical College Qingdao University

Research

Keywords: 125I seeds, lung carcinoma, apoptosis, Ki-67, P21

Posted Date: April 23rd, 2020

DOI: https://doi.org/10.21203/rs.3.rs-23236/v1

Version of Record: A version of this preprint was published at Radiation Oncology on October 15th, 2020.
See the published version at https://doi.org/10.1186/s13014-020-01682-5.

Abstract

Background: Lung cancer is a fatal disease and a serious health problem worldwide. Patients are usually diagnosed at an advanced stage, with the effectiveness of chemotherapy for such patients being very limited. Iodine 125 seed(^{125}I) irradiation can be used as an important adjuvant treatment for lung carcinoma. The purpose of this study was to examine the effects of irradiation by 125I seeds in human lung cancer xenograft model and to determine the underlying mechanisms involved, with a focus on apoptosis.

Methods: A group of 40 mice bearing A549 lung adenocarcinoma xenografts were randomly divided into 4 groups: control group (n=10), sham seed (0 mCi) implant group (n=10), 125I seed (0.6 mCi) implant group (n=10) and 125I seed (0.8 mCi) implant group (n=10), respectively. The body weight and tumor volume, was recorded every four days until the end of the study. Apoptotic cells were checked with terminal deoxynucleotidyl transferase dUTP nick end labeling (TUNEL) assay and activities of caspase-3 and caspase-8 enzyme were tested. Expression of P21, survivin, livin, caspase-9 and proliferating cell nuclear antigen (Ki-67) was detected with immunohistochemical staining.

Results: The results of TUNEL staining assays shows that 125I seed irradiation suppresses the growth of lung cancer xenografts in nude mice and induces apoptosis. The activity of caspase-3 and caspase-8 was significantly higher. The expression levels Ki67, survivin and livin were substantially downregulated, while P21 and caspase-9 protein expression was significantly increased following 125I seed irradiation. This study revealed that 125I seed irradiation could significantly change apoptosis-related protein in human lung cancer xenograft.

Conclusions: Overall, our study demonstrates that radiation exposure by 125I seeds has been expected as a new treatment option for lung cancer.

Background

Primary lung cancer is the most common malignancies(1) and the leading cause of tumorassociated mortality(2–8) in gender-independent populations. Approximately 1.8 million new examples are diagnosed and near 1.6 million fatal cases were estimated annually worldwide, accounting for 19.4% of total cancer mortality, and the total 5-year survival rate was less than 20%(2, 5, 7, 9–12) Non-small cell lung cancer (NSCLC) accounts for approximately 85% of lung cancer and small cell lung cancer (SCLC) was about 15%(3, 4, 6, 13–15), which more than 50% NSCLC is adenocarcinoma(2, 7).Surgery remains the main curative selection for patients with early-stage non-small cell lung cancer. However, in NSCLC patients with advanced disease has not been diagnosed, fewer than 20% of patients can be cured by surgical resection (16). Chemotherapy and radiotherapy (RT) are commonly used for patients who are not considered surgical candidates. However, these modalities are not usually curative and are almost always accompanied by various toxic complications (myelosuppression, nausea, vomiting and radiation pneumonitis), especially affecting important organs and tissues (heart, esophagus, and large blood

vessels)(17, 18). Therefore, it is necessary to effectively prolong the survival time and significantly improve the quality of life in patients with advanced.

125I brachytherapy has been accepted as a minimally and useful invasive treatment for different tumors with significant efficacy. Compared with conventional external radiotherapy, 125I brachytherapy features minimal complications, minimal invasive,high dosage in the diseased area, and a paucity of normal tissues exposed(19–21). It further improves the anti-tumor effect via killing tumor cells and most effectively protects normal tissue (21, 22), and therefore has been rapidly applied in clinic. The most common application of 125I seeds irradiation has been in the local treatment of advanced and inoperable prostate cancer(23, 24), although therapy for other sites of disease, such as lung cancer, hepatocellular carcinoma, gastric carcinoma, colorectal cancer, pancreatic adenocarcinoma and head/neck cancer (19–21, 25–33).

Although many clinical trials have reported that 125I seed radiation is a feasible adjuvant treatment to control local symptoms and prolong survival for advanced or inoperable NSCLC(28, 33), its underlying molecular mechanisms and biological effects are far from fully understood.

Materials And Methods

Cell culture

The human lung adenocarcinoma cell line A549 was purchased from the American Type Culture Collection (ATCC, Manassas, VA, USA). The cells were cultured in RPMI-1640 (Hyclone, Logan, UT) medium supplemented with 10% Fetal Bovine Serum (FBS) (Gibco, Carlsbad, CA, USA) and 1% penicillin-streptomycin (Hyclone) in a 37 °C incubator with 5% CO_2. All procedures were carried out using cells were seeded at 70–80% confluence. Cells were > 95% viable as by staining the cells with Trypan blue for the experiments in vivo.

Animal Model

Female BALB/c nude mice, weighing 17–20 g and 4–6 weeks old, were purchased from Institute of Chinese Academy of Medical Sciences. Before any intervention was initiated, the nude mice were maintained in pathogen-free conditions (55 ± 5% humidity and 23 ± 2℃) for 1 week. The study was approved by animal ethics committee of the University of Qingdao. Nude mice were injected with 5×10^6 A549 cells. Tumor size, volume and weight of the mice were calculated daily until the remainder of the experiment. We calculated the tumor volume (V) using the formula: V (mm^3) = $L \times W^2/2$(W, width of tumor; L, length of tumor).

125i Brachytherapy Seeds Implant

The ^{125}I seeds (4.5 mm long, 0.8 mm diameter) were obtained from Qingdao University Hospital. The energy of ^{125}I was an average from 27.4 to 35.5 keV, and its half-life is about 59.6 days. The ^{125}I were continuously-releasing soft X-ray and low-dose-rate γ-irradiation after decaying into the organs. It is a considerably long of internal radiation, brachytherapy dose (93–97%) was depleted in 8–10 months. Once the tumors had reached 300 mm^3 in size (about 24 days), mice were randomly divided into 4 groups (n = 10/group): sham seed implant group; 125I seed (0.6 mCi) implant group; 125I seed (0.8 mCi) implant group and non-implanted control group. Before cell inoculation, BALB/c nude mice were anesthetized with diethyl ether. The seeds in the form of 18-gauge needles called Mick-applicator directly into the visible tumor of mice. Mice were killed, and tumors from each group were harvested and weighed, then fixed with 4% paraformaldehyde (PFA) after 32 days of treatment.

Hematoxylin And Eosin (h&e) Staining

Tumor tissues were fixed in 4% paraformaldehyde for 24 h. After paraffin imbedding, the tissues were sliced into 4 μm-thick sections. The sections were dehydrated with gradient ethanol, and then stained with hematoxylin for 5 min. After differentiated in 1% hydrochloric acid alcohol for 2 s, the sections were then incubated in ammonia water, followed by the staining with eosin. Ultimately, the sections were dehydrated, cleared, mounted with neutral resin, and observed under light microscopy (Olympus, Japan).

Tunel Staining

Tumor specimens were subjected to a TUNEL assay using the In Situ Cell Death Detection kit (Roche, Basel, Switzerland), according to manufacturer's instructions for detecting apoptosis. As noted above, the fixed tissues were incubated with 100 μl Proteinase K for 30 min at 37 °C. Slides were rinsed twice with PBS. Fifty microliter TUNEL reaction mixture was added to the sample at 37℃ in a humid and dark atmosphere incubated for 60 min.Then fifty microliter Converter-POD solution was added to the sample at 37℃ incubated for 30 min. DAB substrate was added to the slides, overlaid with a coverslip and analyzed under light microscope.

The numbers of overall tumor and TUNEL positive cells were quantified by light microscope at magnification of 400X in five random sections. The apoptotic index was determined as the percentage of TUNEL positive cells to overall tumor cells. Slides with DAB-stained were analyzed by an Olympus BX51TPHD-J11 microscope (Tokyo, Japan). The analysis software (Image Pro Plus, Media Cybernetics, USA) was used for image capture and analyze.

Caspase-3 And Caspase-8 Activity Test

caspase-3 and caspase-8 activity was measured using the caspase-3 and caspase-8 assay kit (Beyotime, Shanghai, China) according to the manufacturer’s protocol. The treated cell lysates were incubated with

chilled lysis buffer on ice for 15 min. Then they were centrifuged (13,000 × g, 4 ◦C, 5 min) and the supernatants were transferred to 96-well plates. Reaction buffer, containing 10 mM DTT was added to each well and the 10 µl Ac-DEVD-*p*NA (2 mM) substrate was mixed. The mixture was incubated for 2 h at 37 ◦C before protease activity was detected using a fluorescence microplate reader at 450 nm.

Immunohistochemistry For P21, Survivin Livin And Caspase-9

Expression of P21, Survivin, Livin and Caspase-9 was detected by Immunohistochemistry. Three sections were tanked from each xenograft tumors. The main procedures are as follows: after conventional deparaffinization, rehydration, and blocking of endogenous peroxidase activity for 15 min, sections were pretreated for the purpose of antigen retrieval by microwaving, and then washed with PBS. Sections were incubated for 2 h at room temperature with mouse anti-human P21 monoclonal antibody (Zsbio, Beijing, China), rabbit anti-human Caspase-9 monoclonal antibody at a 1:50 dilution (Bioss, Beijing, China), rabbit anti-human Survivin monoclonal antibody (Zsbio, Beijing, China) Company) and rabbit anti-human Livin monoclonal antibody at a 1:50 dilution (Bioss, Beijing, China) respectively. Sections were then washed three times in PBS and incubated for 15 min at room temperature with ready-to-use secondary biotinylated antibodies PV-9000. After this, sections were rinsed with PBS, developed with DAB, counterstained with hematoxylin, cleared with xylene and observed under light microscope. Negative control was designed by using PBS instead of primary antibody and a known positive section was served as a positive control. All above mentioned procedures were performed in the same conditions.

Two investigators evaluated the IHC-stained tissue sections and photographed representative regions with Kawasaki et al(34) using a microscope. A mean percentage of positive tumor cells was determined in at least five areas at ×400 and assigned to one of five of categories: (a) 0, <5%; (b) 1,5-25%; (c) 2. 25-50%; (d) 3, 50-75%; and (e) 4. >75%. According to cell staining intensity score: (a) cell no color, 0 points; (b) straw colored, 1 point; (c) brownish-yellow, 2 points; (d)tan, 3 points. According to these indicators divided into four, that is negative for the 0-1 points, weak positive 2-3 points, positive 4-5 points, strong positive 6-7 points.

Statistical analysis

All experiments were performed in three parallels and repeated at least thrice. All data were conducted using SPSS 22.0 software (IBM, Cary, NC, USA). Continuous variables were examined for normality. Results are presented as mean ± standard deviation (SD). Data did pass tests of equal variance. Multiple group comparisons were evaluated by one-way ANOVA. Comparison of means were made by Student-Newman-Keuls test. Differences in proportions were evaluated by chi-square test. Correlations were analyzed by the Spearman rank-correlation coefficient. Difference with $P < 0.05$ were considered statistically significant.

Results

Effect of 125I seed irradiation on tumor growth of lung cancer

We evaluated the antitumor effects of the 125I seeds by A549 cells tumor xenografts of human lung adenocarcinoma. Tumor xenografts were established subcutaneously in 40 nude mice. When the tumors reached a mean volume of 250–350 mm^3 without ischaemic necrosis after 3 weeks,we initiated experiments. After 30 days, the mice were euthanized and tumors were analyzed, all mice survived without cachexia and severely radiation damage. There was no obvious hemorrhagic necrosis and fibrosis of heart, lungs, spleen, liver, and kidneys. All particles were located near the middle of the tumor xenografts, and successfully recovered.

In the case of xenograft tumors, median volume was 886 mm^3 ± 97 in the in the 0.6 mCi group and 590 mm^3 ± 107 in the 0.8 mCi group, which was difference($P < 0.001$) compared with the controls (2297 mm^3 ± 149).There was no significant difference in the 0 mCi(1779 mm^3 ± 276) and control group($P > 0.05$). The 0.6 mCi groups were no different from 0.8 mCi group($P > 0.05$).

The weight of nude mice remained at steady state after particle implantation in all groups. However, the weight declined in the mice of 0.6 and 0.8 mCi groups over time, and there was no difference which compared with the control group ($P > 0.05$).

The weight of nude mice in the 0.6 and 0.8 mCi groups was less than the control group on the 30th day ($P < 0.05$), but there was no significant difference between the 0.6 and the 0.8 mCi group, 0 mCi and the control group ($P > 0.05$).

The tumor weights in the 0.6 mCi(1.20 ± 0.44)g and 0.8 mCi(0.99 ± 0.404)g groups were less than the control group(2.35 g ± 0.64, $P < 0.05$ for all comparisons).

A comparison between 0.8 mCi and 0.6 mCi group was no significant($P > 0.05$). There was no statistically significant difference between 0 mCi and the control group ($P > 0.05$). The growth inhibition of tumor was 49% in 0.6 mCi group and 62% in 0.8 mCi group.

Histopathological Alterations In Xenograft Tumors

Hematoxylin and eosin (H&E) stained sections shows the tumor cells as red, the blood vessels and the stroma blue. Sections were stained with H&E which observed abundant tumor cells and stroma. The tumor cells with closely packed, ill-defined vague outlines, active growth, larger and darker-staining nuclei, numerous mitoses, abundant blood vessels, minimal or no liquefaction necrosis in the 0 mCi and the control group (Fig. 1). The tumor cells were massive necrosis,homogeneous, red discoloration in the 0.6 mCi and 0.8 mCi groups. The normal cellular structure was basically invisible. The remaining cancer

cells adjacent areas of necrosis were loosely arranged, karyolysis, no significant cytoplasmic staining, eosinophilic. Adjacent blood vessels were reduced, angiogenesis was not common (Fig. 1).

Effect Of I Radiation On Proliferation And Apoptosis

Ki-67 was stained for nuclei, positive staining for cells was brown or tan in 0.6 and 0.8 mCi groups, mainly in the form of spots or lumps. These results indicate that low level and lighter brown of cells in 0.6 and 0.8 mCi groups, and more positive staining for cells and deeply brown in 0 and control groups (Fig. 2). We calculated the proliferation index of the tumor cells (Table 1). The proliferation index was substantially reduced in the 0.6 and 0.8 mCi groups than the control group ($P < 0.05$). However, no statistically significant difference was found between the 0.6 and 0.8 mCi groups ($P > 0.05$). The comparison between 0 mCi and control group was also no difference ($P > 0.05$). Here we show that 125I particles brachytherapy remarkably inhibits tumor cell proliferation.

Table 1
Proliferative index and apoptosis index expression in tumors (`x±)%

group	n	proliferative index(%)	apoptosis index(%)
control group	10	71.00 ± 10.00	27.00 ± 4.69
0 mCi group	10	63.20 ± 6.22	35.50 ± 3.42
0.6 mCi group	10	46.20 ± 8.35*	50.00 ± 2.58*
0.8 mCi group	10	38.60 ± 6.03*	62.33 ± 4.51*
F value		31.853	45.34
P value		0.001	0.001
Note: Compared with the control group, *P** 0.05			

Under light microscope, nuclear staining of apoptotic cells was in yellow-brown by TUNEL. The number of apoptotic cells in 0.8 mCi group and 0.6 mCi group were significantly higher than those in 0 and control group (Figure.3). Compared with the control mice, the 0.6 and 0.8 mCi groups had significantly higher apoptotic index ($P < 0.05$). The differences were not statistically significant between 0 mCi group and controls ($P > 0.05$). A comparison of the 0.6 mCi group and 0.8 mCi groups that had no difference ($P > 0.05$). We examined the activity of caspase-3 and caspase-8 (Table 2). The activity of caspase-3 and caspase-8 in 0.6 mCi and 0.8 mCi groups was significantly higher than control group ($P < 0.05$). There was no significant difference between groups of 0 mCi and control ($P > 0.05$). The difference between 0.6 mCi and 0.8 mCi groups was not significant ($P > 0.05$). These results suggest that ^{125}I implanted radiotherapy can significantly accelerated tumor cell apoptosis.

Table 2
Expression of caspase-3 and caspase-8 activities in tumors in each group (`x±)%

group	n	caspase-3	caspase-8
control group	10	0.23 ± 0.03	0.32 ± 0.03
0 mCi group	10	0.21 ± 0.23	0.34 ± 0.12
0.6 mCi group	10	0.67 ± 0.12*	0.83 ± 0.49*
0.8 mCi group	10	0.70 ± 0.12*	1.15 ± 0.17*
F value		621.383	11.57
P value		0.001	0.001
Note: Compared with the control group,*P** 0.05			

Expression Of P21, Caspase-9, Survivin, Livin Proteins

After treatment in the animals of all four groups, we determined the P21, survivin, livin and caspase-9 protein expression in A549 xenograft tumors by immunohistochemistry (Figure. 4,5,6,7). The positive rate P21, survivin, livin and caspase-9 protein expression in four groups was calculated (Table 3). In groups 0.6 mCi and 0.8 mCi, the positivity rate of P21 and caspase-9 protein expression was significantly higher compared to the control group ($P < 0.05$), while survivin and livin markedly lower than in control group ($P < 0.05$). There was no statistically significant difference in the expression of P21, caspase-9, survivin and livin between the 0 mCi group and the controls ($P > 0.05$). The four proteins were not different between the groups 0.6 mCi and 0.8 mCi ($P > 0.05$).

Table 3
Protein expression in tumors (`x±)%

group	n	Protein expression			
		P21	Caspase-9	Survivin	Linvin
control group	10	16. 7%	33.3%	77.8%	83.3%
0 mCi group	10	22.2%	38.9%	66.7%	77.8%
0.6 mCi group	10	66.7%*	77.8%*	27.8%*	33.3%*
0.8 mCi group	10	88.9%*	88.7%*	6%*	16.7%*
Note: Compared with the control group,*P** 0.05					

Discussion

Despite significant advancements in surgery, radiotherapy, and chemotherapy have been forged in recent years, yet rate of survival at 5 year survival remains poor. The role of radiation therapy in the treatment, plays an important role of advanced stage non-small-cell lung cancer. Interstitial brachytherapy with radioactive seeds has a history spanning more than 100 years. The anti-tumor effect of 125I seed has been studied in recent years, as well as the mechanism of 125I seed for induction of apoptosis and cell cycle inhibition(19, 20, 27–29, 33, 35), DNA hypomethylation(19, 30) and anti-angiogenesis(27, 36, 37). The most extensively studied mechanism is apoptosis. More recently, studies have shown that apoptosis and inhibiting proliferation may play an essential role in the treatment effects of ^{125}I, but their mechanism of action has not been determined completely. Blocking in apoptosis may confer a survival advantage on malignant cells harboring genetic alterations and thus promote cancer progression(38). It is likely that mitochondrial related autophagy disturbed mitochondria-dependent apoptotic pathway to delay apoptosis(39). In radiation therapy, radiation can induce autophagy in normal and cancer cells(40–43).

Survivin is a well-known protein that belongs to the family of the inhibitor of apoptosis proteins (IAP) family which can regulate of tumor cell division and apoptosis inhibition. It is encoded by the BIRC5 gene located on the chromosome 17q25 (44). Livin has been identified as a new member of the IAP family which was first identified in melanoma samples and was named melanoma inhibitor of apoptosis(45). Livin, a member of the inhibitors of apoptosis proteins, is overexpressed in tumor tissues and is detected at substantially lower levels or not expressed at all in corresponding normal tissues. Its expression is considered a poor prognostic marker.(38, 46). P21 is one of the most important negative regulatory factors in the cell cycle and also plays a very important role in the process of apoptosis and cell proliferation(47–49). P21 mainly regulate the activity of intracellular CDK (cyclin dependent kinase) leaving the cells in the G1 or G2 phase(47–49), through the regulation of tumor suppressor gene p53, but also by p53-dependent manner by other factors induced by the production. Ki67 have been described as a reliable indicator in the rate of cell proliferation, which is a proliferation marker expression in cells expression throughout all stages except G0 phase(45).

The central event in apoptosis is the proteolytic activation of a class of cysteine aspartyl-specific proteases(Caspase) family(38, 45, 50–55). Caspases are known to act as important mediators of apoptosis and contribute to the overall apoptotic morphology by the cleavage of various cellular substrates(44, 49, 54). Caspase-3 is an important regulator of apoptosis and key enzyme in the Caspase family, and most factors initiate apoptosis through caspase − 3-mediated pathway(37, 44). Caspase-3 is the main performer of the apoptotic procedure, activating DNA fragments, leading to DNA degradation, resulting in nuclear fragmentation and inducing apoptosis by cascade reactions(38). This gene encodes a protein that belongs to a highly conserved family of cysteinyl aspartate-specific proteases that function as essential regulators of programmed cell death through apoptosis. The increase of caspase-3 expression may induce the mitochondria-dependent apoptotic pathway with the possible mitochondria-independent pathway for the caspase-8 activation for that caspase-8-mediated apoptosis induced by oxidative stress is independent of the intrinsic pathway and dependent on cathepsins(38, 45, 50–55). The

intrinsic pathway of apoptosis is associated with the activation of caspase-9, which cleaves and activates caspase-3(49–54).

We investigated the mechanism of 125I seed in treating lung cancers by establishing and using an animal transplant tumor model. Our results demonstrated that a higher absorbed dose of 125I induced a higher percentage of apoptosis. The results confirmed that 125I treatment induced tumor cell apoptosis, with decreasing P21, Ki-67, survivin, livin level expression, growing Caspase-9 expression and elevated caspase-3 activation. Implantation of 125I particles resulted in a decrease of Ki-67 expression in the tumor, thereby inhibiting cell proliferation. P21, survivin and livin all can affect apoptosis by inhibiting caspase-3 at the same time. Livin is recruited to death receptor signaling complexes, where it inhibits activation of caspases responsible for apoptosis and protects cells from diverse pro-apoptotic stimuli(38, 45). Livin interacts with downstream caspases, such as caspase-3 and caspase-9, leading to their inactivation and degradation(45). It has been suggested that antisense oligonucleotide of livin could promote cancer cell apoptosis by increasing the caspase-3-mediated apoptosis pathway(38, 45).

Moreover, p21 shields the cancer cells from death induced by DNA-damaging agents, and altered p21 expression increases sensitivity to treatment in vivo(47, 49). P21 is an apoptosis regulatory factor, which is due to inhibition of the activity of procaspase-3(48). The antiapoptotic effect of survivin is connected with the activation of caspase-3. Survivin can directly inhibit the activity of caspase-3 in downstream of apoptotic pathway and indirectly inhibit the activation of caspase-3 by caspase-9(50–55). The tumor xenografts after 125I radiation treatment, the expression of survivin and livin protein decreased, while the expression of P21 increased. The effect of all three on caspase-3 was weakened at the same time, which inhibited the activity and function of caspase-3 and promoted the apoptosis of A549 cells.

In conclusion, our study successfully establishes the mouse lung adenocarcinoma model and provides a beneficial exploration of radiobiology of continuous different dose 125I seed irradiation in the treatment of lung adenocarcinoma. 125I seed implantation effectively inhibited tumor growth and reduced tumor volume, thus reducing tumor volume and improving the quality of animal survival. 125I irradiation inhibited the proliferation and induced apoptosis is the key mechanisms underlying the therapeutic effect of 125I seed implantation. In the tumor microenvironment, 125I irradiation can inhibit cell proliferation by reducing the levels of Ki-67, as well as inducing apoptosis by increasing the level of P21 and reducing the levels of survivin and livin. Although the mechanism of 125I particles in the treatment of tumors is not completely elucidated and many problems remain to be addressed, with further development of fundamental research, the application of 125I seed implantation in clinical practice will continue to be improved in order to be better applied in clinical practice.

Abbreviations

Ki- 67, nuclcar- associated antigen

P21, protein 21

Caspse, cysteine aspartyl-specific proteases

NSCLC, Non-small cell lung cancer

SCLC, small cell lung cancer

H&E, Hematoxylin and eosin

TUNEL, terminal deoxynucleotidyl transferase-mediated biotinylated UTP nick end labeling

DAB, diaminobenzidine

IHC, immunohistochemistry

IAP, inhibitor of apoptosis proteins

Declarations

Ethics approval and consent to participate

The study was approved by our university's animal experiment review committee, and all animal experiment procedures were performed in accordance with the guidelines for animal care and use.

Competing interests

The authors declare that they have no known competing financial interests or personal relationships that could have appeared to influence the work reported in this paper.

Funding

This study was supported by the Key Laboratory of Marine Drug, Ministry of Education (KLMDOUC201307)

Authors' contributions

QJ was responsible for the conception of the study and drafted the manuscript. CL, XZ, YC, CG and LW were responsible for data acquisition and analysis; CL and LW revised and commented on the draft; all authors read and approved the final version of the manuscript.

Acknowledgements

Not applicable.

Availability of data and materials

The datasets used and/or analyzed during the current study are available from the corresponding author on reasonable request.

Consent for publication

All the authors agreed to publish this manuscript.

References

1. Mizugaki H, Yamamoto N, Nokihara H, Fujiwara Y, Horinouchi H, Kanda S, et al. A phase 1 study evaluating the pharmacokinetics and preliminary efficacy of veliparib (ABT-888) in combination with carboplatin/paclitaxel in Japanese subjects with non-small cell lung cancer (NSCLC). Cancer chemotherapy and pharmacology. 2015;76(5):1063-72.
2. Deneka AY, Haber L, Kopp MC, Gaponova AV, Nikonova AS, Golemis EA. Tumor-targeted SN38 inhibits growth of early stage non-small cell lung cancer (NSCLC) in a KRas/p53 transgenic mouse model. PloS one. 2017;12(4):e0176747.
3. Scrima M, Zito Marino F, Oliveira DM, Marinaro C, La Mantia E, Rocco G, et al. Aberrant Signaling through the HER2-ERK1/2 Pathway is Predictive of Reduced Disease-Free and Overall Survival in Early Stage Non-Small Cell Lung Cancer (NSCLC) Patients. Journal of Cancer. 2017;8(2):227-39.
4. Kolokotroni E, Dionysiou D, Veith C, Kim YJ, Sabczynski J. In Silico Oncology: Quantification of the In Vivo Antitumor Efficacy of Cisplatin-Based Doublet Therapy in Non-Small Cell Lung Cancer (NSCLC) through a Multiscale Mechanistic Model. 2016;12(9):e1005093.
5. Kudinov AE, Deneka A. Musashi-2 (MSI2) supports TGF-beta signaling and inhibits claudins to promote non-small cell lung cancer (NSCLC) metastasis. 2016;113(25):6955-60.
6. Vazquez S, Casal J, Afonso Afonso FJ, Firvida JL, Santome L, Baron F, et al. EGFR testing and clinical management of advanced NSCLC: a Galician Lung Cancer Group study (GGCP 048-10). Cancer management and research. 2016;8:11-20.
7. Whang YM, Park SI, Trenary IA, Egnatchik RA, Fessel JP, Kaufman JM, et al. LKB1 deficiency enhances sensitivity to energetic stress induced by erlotinib treatment in non-small-cell lung cancer (NSCLC) cells. Oncogene. 2016;35(7):856-66.
8. Rudisch A, Dewhurst MR, Horga LG, Kramer N, Harrer N, Dong M, et al. High EMT Signature Score of Invasive Non-Small Cell Lung Cancer (NSCLC) Cells Correlates with NFkappaB Driven Colony-Stimulating Factor 2 (CSF2/GM-CSF) Secretion by Neighboring Stromal Fibroblasts. PloS one. 2015;10(4):e0124283.
9. Gridelli C, Camerini A, Pappagallo G, Pennella A, Anzidei M, Bellomi M, et al. Clinical and radiological features driving patient selection for antiangiogenic therapy in non-small cell lung cancer (NSCLC). Cancer imaging : the official publication of the International Cancer Imaging Society. 2016;16(1):44.
10. Barnfield PC, Ellis PM. Second-Line Treatment of Non-Small Cell Lung Cancer: New Developments for Tumours Not Harbouring Targetable Oncogenic Driver Mutations. Drugs. 2016;76(14):1321-36.

11. Hong QY, Wu GM, Qian GS, Hu CP, Zhou JY, Chen LA, et al. Prevention and management of lung cancer in China. Cancer. 2015;121 Suppl 17:3080-8.
12. Zhang X, Liu S, Liu Y, Du J, Fu W, Zhao X, et al. Economic Burden for Lung Cancer Survivors in Urban China. International journal of environmental research and public health. 2017;14(3).
13. Castanon E, Rolfo C, Vinal D, Lopez I, Fusco JP, Santisteban M, et al. Impact of epidermal growth factor receptor (EGFR) activating mutations and their targeted treatment in the prognosis of stage IV non-small cell lung cancer (NSCLC) patients harboring liver metastasis. Journal of translational medicine. 2015;13:257.
14. Lee SO, Yang X, Duan S, Tsai Y, Strojny LR, Keng P, et al. IL-6 promotes growth and epithelial-mesenchymal transition of CD133+ cells of non-small cell lung cancer. Oncotarget. 2016;7(6):6626-38.
15. Jung JH, Kim MJ, Lee H, Lee J, Kim J, Lee HJ, et al. Farnesiferol c induces apoptosis via regulation of L11 and c-Myc with combinational potential with anticancer drugs in non-small-cell lung cancers. Scientific reports. 2016;6:26844.
16. Toyokawa G, Takenoyama M, Ichinose Y. Multimodality treatment with surgery for locally advanced non-small-cell lung cancer with n2 disease: a review article. Clinical lung cancer. 2015;16(1):6-14.
17. Liew MS, Sia J, Starmans MH, Tafreshi A, Harris S, Feigen M, et al. Comparison of toxicity and outcomes of concurrent radiotherapy with carboplatin/paclitaxel or cisplatin/etoposide in stage III non-small cell lung cancer. Cancer medicine. 2013;2(6):916-24.
18. Cannon DM, Mehta MP, Adkison JB, Khuntia D, Traynor AM, Tome WA, et al. Dose-limiting toxicity after hypofractionated dose-escalated radiotherapy in non-small-cell lung cancer. Journal of clinical oncology : official journal of the American Society of Clinical Oncology. 2013;31(34):4343-8.
19. Ma JX, Jin ZD, Si PR, Liu Y, Lu Z, Wu HY, et al. Continuous and low-energy 125I seed irradiation changes DNA methyltransferases expression patterns and inhibits pancreatic cancer tumor growth. Journal of experimental & clinical cancer research : CR. 2011;30:35.
20. Ma ZH, Yang Y, Zou L, Luo KY. 125I seed irradiation induces up-regulation of the genes associated with apoptosis and cell cycle arrest and inhibits growth of gastric cancer xenografts. Journal of experimental & clinical cancer research : CR. 2012;31:61.
21. Wang H, Wang J, Jiang Y, Li J, Tian S, Ran W, et al. The investigation of 125I seed implantation as a salvage modality for unresectable pancreatic carcinoma. Journal of experimental & clinical cancer research : CR. 2013;32:106.
22. Connell T, Alexander A, Papaconstadopoulos P, Serban M, Devic S, Seuntjens J. Delivery validation of an automated modulated electron radiotherapy plan. Medical physics. 2014;41(6):061715.
23. Mohler JL, Armstrong AJ, Bahnson RR, Boston B, Busby JE, D'Amico AV, et al. Prostate cancer, Version 3.2012: featured updates to the NCCN guidelines. Journal of the National Comprehensive Cancer Network : JNCCN. 2012;10(9):1081-7.
24. Ferreira AS, Guerra MR, Lopes HE, Lima UT, Vasconcelos YA, Teixeira MT. Brachytherapy and radical prostatectomy in patients with early prostate cancer. Revista da Associacao Medica Brasileira

(1992). 2015;61(5):431-9.

25. Jiang YL, Meng N, Wang JJ, Ran WQ, Yuan HS, Qu A, et al. Percutaneous computed tomography/ultrasonography-guided permanent iodine-125 implantation as salvage therapy for recurrent squamous cell cancers of head and neck. Cancer biology & therapy. 2010;9(12):959-66.
26. Qin QH, Huang BS, Tan QX, Yang WP, Lian B, Wei CY. Radiobiological effect induced by different activities of (125)I seed brachytherapy in a hepatocellular carcinoma model. International journal of clinical and experimental medicine. 2014;7(12):5260-7.
27. Ma Z, Yang Y, Yang G, Wan J, Li G, Lu P, et al. Iodine-125 induces apoptosis via regulating p53, microvessel density, and vascular endothelial growth factor in colorectal cancer. World journal of surgical oncology. 2014;12:222.
28. Cheng J, Ma S, Yang G, Wang L, Hou W. The Mechanism of Computed Tomography-Guided 125I Particle in Treating Lung Cancer. Medical science monitor : international medical journal of experimental and clinical research. 2017;23:292-9.
29. Wang H, Li J, Qu A, Liu J, Zhao Y, Wang J. The different biological effects of single, fractionated and continuous low dose rate irradiation on CL187 colorectal cancer cells. Radiation oncology (London, England). 2013;8:196.
30. Yang Y, Ma ZH, Li XG, Zhang WF, Wan J, Du LJ, et al. Iodine-125 irradiation inhibits invasion of gastric cancer cells by reactivating microRNA-181c expression. Oncology letters. 2016;12(4):2789-95.
31. Liu K, Ji B, Zhang W, Liu S, Wang Y, Liu Y. Comparison of iodine-125 seed implantation and pancreaticoduodenectomy in the treatment of pancreatic cancer. International journal of medical sciences. 2014;11(9):893-6.
32. Yu YP, Yu Q, Guo JM, Jiang HT, Di XY, Zhu Y. Effectiveness and security of CT-guided percutaneous implantation of (125)I seeds in pancreatic carcinoma. The British journal of radiology. 2014;87(1039):20130642.
33. Wang Z, Zhao Z, Lu J, Chen Z, Mao A, Teng G, et al. A comparison of the biological effects of 125I seeds continuous low-dose-rate radiation and 60Co high-dose-rate gamma radiation on non-small cell lung cancer cells. PloS one. 2015;10(8):e0133728.
34. Kawasaki H, Altieri DC, Lu CD, Toyoda M, Tenjo T, Tanigawa N. Inhibition of apoptosis by survivin predicts shorter survival rates in colorectal cancer. Cancer research. 1998;58(22):5071-4.
35. Sachs RK, Chen AM, Brenner DJ. Review: proximity effects in the production of chromosome aberrations by ionizing radiation. International journal of radiation biology. 1997;71(1):1-19.
36. Xiang GL, Zhu XH, Lin CZ, Wang LJ, Sun Y, Cao YW, et al. 125I seed irradiation induces apoptosis and inhibits angiogenesis by decreasing HIF-1alpha and VEGF expression in lung carcinoma xenografts. Oncology reports. 2017;37(5):3075-83.
37. Chen F, Wang D. Inhibition of glioblastoma growth and invasion by 125I brachytherapy in rat glioma model. Am J Transl Res. 2017;9(5):2243-54.
38. Myung DS, Park YL, Chung CY, Park HC, Kim JS, Cho SB, et al. Expression of Livin in colorectal cancer and its relationship to tumor cell behavior and prognosis. PloS one. 2013;8(9):e73262.

39. Calgarotto AK, da Silva Pereira GJ, Bechara A, Paredes-Gamero EJ, Barbosa CM, Hirata H, et al. Autophagy inhibited Ehrlich ascitic tumor cells apoptosis induced by the nitrostyrene derivative compounds: relationship with cytosolic calcium mobilization. European journal of pharmacology. 2012;678(1-3):6-14.
40. Anbalagan S, Pires IM, Blick C, Hill MA, Ferguson DJ, Chan DA, et al. Radiosensitization of renal cell carcinoma in vitro through the induction of autophagy. Radiotherapy and oncology : journal of the European Society for Therapeutic Radiology and Oncology. 2012;103(3):388-93.
41. Levy JM, Thorburn A. Targeting autophagy during cancer therapy to improve clinical outcomes. Pharmacology & therapeutics. 2011;131(1):130-41.
42. Mancias JD, Kimmelman AC. Targeting autophagy addiction in cancer. Oncotarget. 2011;2(12):1302-6.
43. Yang Z, Xu Y, Xu L, Maccauro G, Rossi B, Chen Y, et al. Regulation of autophagy via PERK-eIF2alpha effectively relieve the radiation myelitis induced by iodine-125. PloS one. 2013;8(11):e76819.
44. Jafari N, Zargar SJ, Yassa N, Delnavazi MR. Induction of Apoptosis and Cell Cycle Arrest by Dorema Glabrum Root Extracts in a Gastric Adenocarcinoma (AGS) Cell Line. Asian Pacific journal of cancer prevention : APJCP. 2016;17(12):5189-93.
45. Xue D, Zuo K, Li X, Zhang T, Chen H, Cheng Y, et al. Expression and prognostic significance of livin, caspase-3, and ki-67 in the progression of human ampullary carcinoma. Applied immunohistochemistry & molecular morphology : AIMM. 2013;21(6):525-31.
46. Yan B. Research progress on Livin protein: an inhibitor of apoptosis. Molecular and cellular biochemistry. 2011;357(1-2):39-45.
47. Yanagi T, Nagai K, Shimizu H, Matsuzawa SI. Melanoma antigen A12 regulates cell cycle via tumor suppressor p21 expression. Oncotarget. 2017;8(40):68448-59.
48. Ko JH, Lee JH, Jung SH, Lee SG, Chinnathambi A, Alharbi SA, et al. 2,5-Dihydroxyacetophenone Induces Apoptosis of Multiple Myeloma Cells by Regulating the MAPK Activation Pathway. Molecules (Basel, Switzerland). 2017;22(7).
49. Rasool RU, Nayak D, Chakraborty S, Faheem MM, Rah B, Mahajan P, et al. AKT is indispensable for coordinating Par-4/JNK cross talk in p21 downmodulation during ER stress. Oncogenesis. 2017;6(5):e341.
50. Weinlander E, Somnay Y, Harrison AD, Wang C, Cheng YQ, Jaskula-Sztul R, et al. The novel histone deacetylase inhibitor thailandepsin A inhibits anaplastic thyroid cancer growth. The Journal of surgical research. 2014;190(1):191-7.
51. Charette N, De Saeger C, Horsmans Y, Leclercq I, Starkel P. Salirasib sensitizes hepatocarcinoma cells to TRAIL-induced apoptosis through DR5 and survivin-dependent mechanisms. Cell death & disease. 2013;4:e471.
52. Tang XP, Tang GD, Fang CY, Liang ZH, Zhang LY. Effects of ginsenoside Rh2 on growth and migration of pancreatic cancer cells. World journal of gastroenterology. 2013;19(10):1582-92.

53. Liu BX, Zhou JY, Li Y, Zou X, Wu J, Gu JF, et al. Hederagenin from the leaves of ivy (Hedera helix L.) induces apoptosis in human LoVo colon cells through the mitochondrial pathway. BMC complementary and alternative medicine. 2014;14:412.
54. Cheung CH, Sun X, Kanwar JR, Bai JZ, Cheng L, Krissansen GW. A cell-permeable dominant-negative survivin protein induces apoptosis and sensitizes prostate cancer cells to TNF-alpha therapy. Cancer cell international. 2010;10:36.
55. Chougule M, Patel AR, Sachdeva P, Jackson T, Singh M. Anticancer activity of Noscapine, an opioid alkaloid in combination with Cisplatin in human non-small cell lung cancer. Lung cancer (Amsterdam, Netherlands). 2011;71(3):271-82.

Figures

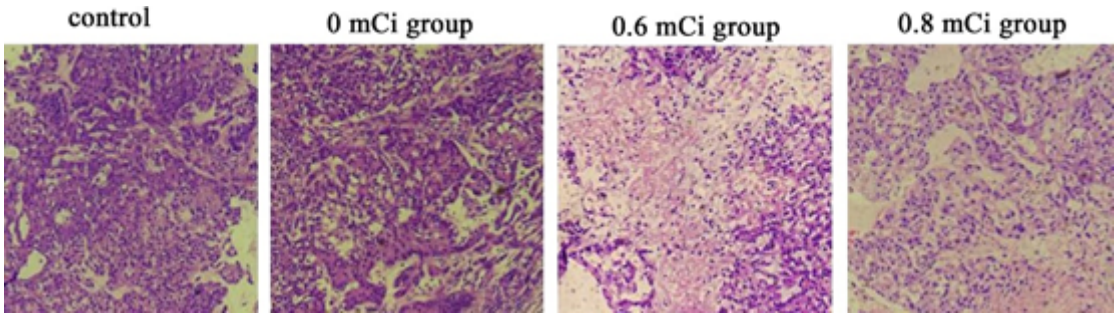

Figure 1

Sections of tumors developing in nude mice stained with HE (×100).

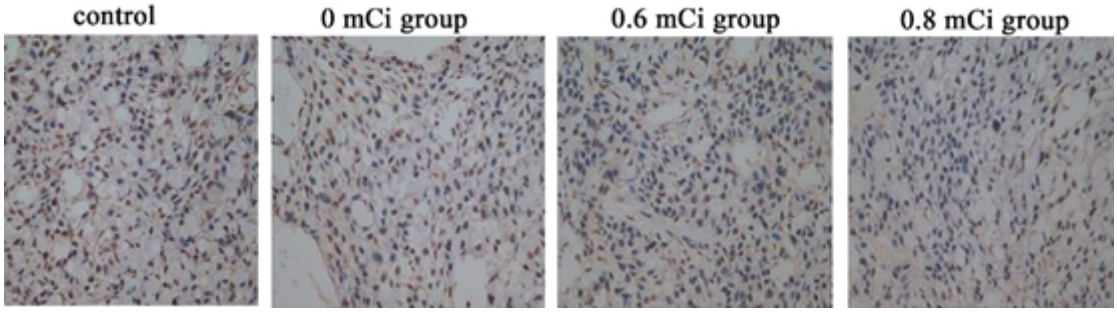

Figure 2

Tumors developing in nude mice stained with anti- Ki-67 monoclonal antibody(x400).

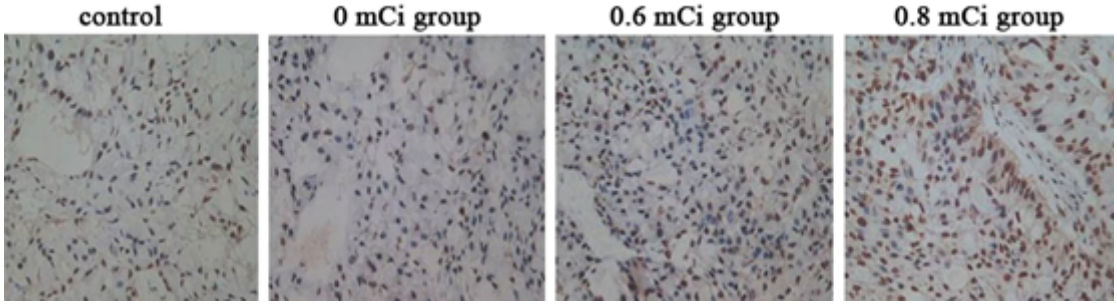

Figure 3

Sections of tumors developing in nude mice stained with TUNEL (×400).

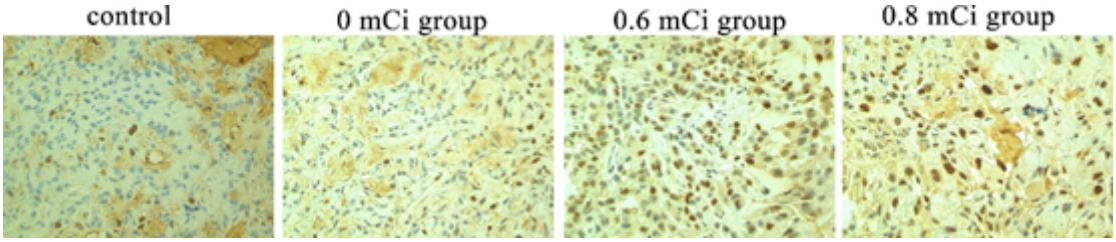

Figure 4

Immunocytochemistry of P21 protein in nude mice xenografts (S-P method × 400)

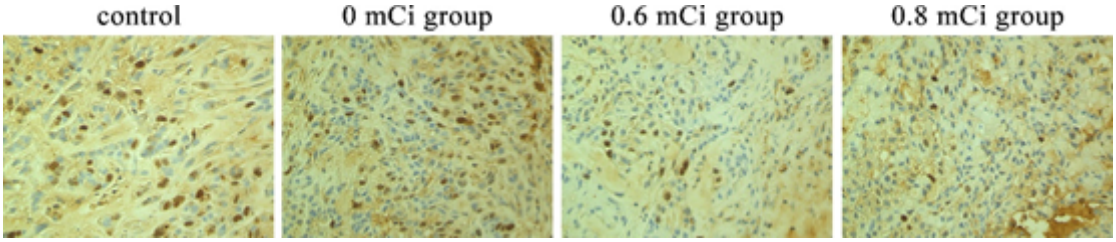

Figure 5

Immunocytochemistry of survivin protein in nude mice xenografts (S-P method × 400)

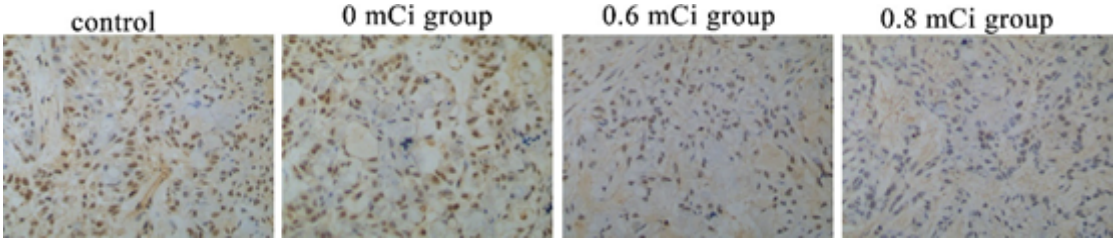

Figure 6

Immunocytochemistry of livin protein in nude mice xenografts (S-P method × 400)

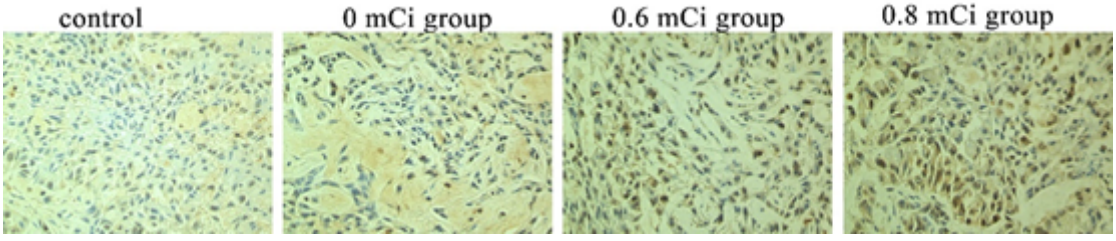

Figure 7

Immunocytochemistry of caspase-9 protein in nude mice xenografts (S-P method × 400)